Practical nonlinear analysis of unreinforced concrete tunnel linings

Vassilis K. Papanikolaou*[a] and Andreas J. Kappos[b]

[a] *Civil Engineering Department, Aristotle University of Thessaloniki, P.O. Box 482, Thessaloniki, 54124, Greece*

[b] *Department of Civil Engineering, City University London, London EC1V OHB, UK.*

Abstract. A comprehensive methodology for modelling, analyzing and assessing the structural response of unreinforced concrete tunnel linings is presented. Various modelling techniques are described, considering the plane finite element representation of the lining geometry, material constitutive laws, and boundary and interface conditions. Furthermore, all relevant external loading cases are studied, including gravity, environmental, fire, blast, and seismic loading. Potential pitfalls in the modelling and analysis procedures are identified and properly dealt with. The suggested methodology is finally applied to actual tunnel linings and the interpretation of the analysis results leads to important conclusions regarding the applicability of different analysis methods and the performance of unreinforced concrete linings.

Keywords: tunnels; concrete; finite elements; modelling; nonlinear analysis.

1. Introduction

Although the lining of modern roadway tunnels is typically constructed in reinforced concrete, cost considerations sometimes lead to the use of unreinforced (plain) concrete when the right conditions are met, mainly when the tunnel is constructed in solid rock and when dynamic loads are not critical for the design of the lining. Notwithstanding cost considerations, the use of plain concrete has the advantage that it relieves construction from the problems associated with the use of reinforcement bars, i.e. compaction of concrete in congested regions and possible damage inflicted to waterproofing membranes by the steel bars.

Unreinforced concrete linings are expected to crack and the extent of cracking is the most critical design criterion in such linings. It is notable that modern design specifications for tunnels, like the German ZTV-ING (BASt, 2007), or the American Technical Manual for Design and Construction of Road Tunnels (FHWA, 2009) do not contain any specific requirements for this case; in fact, allowable crack criteria for unreinforced linings are the subject of current research (see http://www.bast.de/nn_74576/EN/E-Forschungsprojekte/e-laufende/e-fp-laufend-b3.html). Other documents like the French Recommendations for plain concrete in tunnels (AFTES, 2000) adopt indirect criteria for crack control, i.e. they place limits on the residual compression zone, by requiring that the eccentricity of the axial load e = M/N (where M is the bending moment and N the axial load) should not exceed 30% of the lining thickness.

Noticeable differences exist among current codes with respect to the assumptions made for the verification of unreinforced linings against bending moment and axial load, in particular with respect to the way the tensile strength of concrete is taken into account. The European code for concrete, Eurocode 2 (CEN 2004a), includes rather detailed provisions for plain concrete (meant for static loading only) and specifies that tensile strength of concrete can be taken into account; however, the pertinent design equation adopted by Eurocode 2 ignores this strength and only involves the compression strength and the eccentricity (e). The FHWA (2009) Manual requires a check of the tensile stresses (and also the compressive stresses) under the design M and N. Other documents like the AFTES (2000) recommendations ignore the tensile strength of concrete and the basic design verification is a limitation of the eccentricity (see above); a similar procedure is adopted in the German Recommendations for Unreinforced Linings (DAUB 2007). Further discrepancies exist in shear verifications, which are mandatory in some codes (FHWA, Eurocode 2) but are not required in others (DAUB).

[a] Corresponding author, Lecturer. E-mail: billy@civil.auth.gr
[b] Professor. E-mail: Andreas.Kappos.1@city.ac.uk

The above remarks make it clear that there is still substantial room for improving/refining the existing procedures for the design of unreinforced concrete linings. Moreover, the paramount role of parameters like the crack width, which are difficult to estimate reliably using elastic methods, point to the need of using sophisticated methods of analysis, namely nonlinear finite element analysis, as part of the design process of plain concrete linings and/or for calibrating simpler methods for practical design.

The present study is a contribution in this direction, using existing regulations as a starting point for introducing appropriate analysis methods that allow proper checking of the pertinent performance criteria, focussing on deformation quantities. It has to be pointed out here that use of advanced analysis tools (nonlinear finite elements or finite differences) is already part of actual design practice (e.g. Corigliano et al. 2011), at least in important tunnels, and are specifically recognised by pertinent documents like the American FHWA (2009). The present study originated in a very practical context, i.e. the assessment of the capacity of the unreinforced concrete linings proposed by the Constructor's team for parts of three major tunnels (up to 6 km long) currently being built in Greece, and nonlinear finite element analysis was used both by the consultants of the Constructor and by the authors who acted as reviewers of the design of the tunnel linings. The paper attempts to provide proper guidance for the reliable and efficient use of the aforementioned advanced analysis tools by designers with adequate experience in the field. Furthermore, it addresses for the first time the detailed analysis of plain concrete linings subjected to seismic loading, an issue that is typically ignored in previous studies.

2. Modelling procedures

In this section, various techniques for finite element modelling of unreinforced tunnel linings are described, considering geometry, material constitutive laws, and boundary and interface conditions. Furthermore, the relevant load cases will be presented, including gravity, environmental, fire, blast, and seismic loading. Specific numerical values together with corresponding analysis results in an actual application will be presented in the next section. The discussion focuses on two typical cross-section types used in roadway tunnels, nevertheless the modelling approach used can be applied to other cross-sections as well.

Two typical lining cross-section 'prototypes' are considered (Fig. 1), the first of the horseshoe type with strip footings, and the second of the closed type with an invert (typically required in weak rock conditions); the vault geometry is identical in both sections. The outer radius of the vault of the actual sections depicted in Fig. 1, from the centre of the traffic lane, is 7.85 m and the lining thickness is 0.45 m. For modelling and analysis, the finite element package ATENA (Červenka et al. 2012), specifically developed for plain and reinforced concrete structures, is employed throughout the present study.

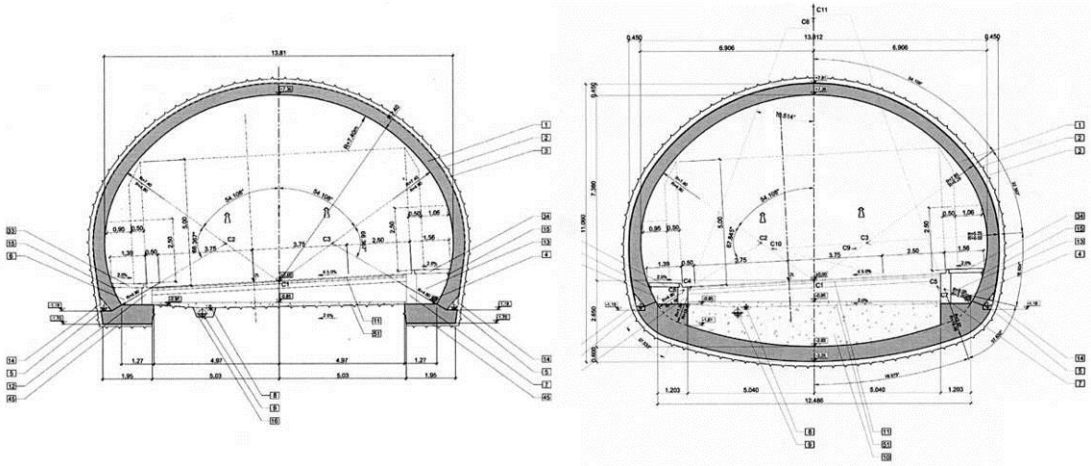

Fig. 1 Typical lining sections : horseshoe (left) and closed section with invert (right). Courtesy of EOAE SA.

2.1 Modelling of the lining section

Following the usual assumption of infinite tunnel length (in reality the length of a tunnel segment is about 14 m), a two-dimensional (2D) finite element formulation under plane strain conditions ($\varepsilon_z = 0$, $\sigma_z \neq 0$) is adopted. Four-node quadrilateral finite elements with typical size of 7.5 cm and thickness of 1.0 m are utilized, leading to a dense mesh of a total of 2538 and 4050 elements (6 elements across lining thickness) for the horseshoe and invert geometries, respectively (Fig. 2). The mesh density is selected with a view to striking a balance between (a) adequate resolution in analysis results and (b) heavy computational requirements, considering the use of advanced nonlinear material models and boundary conditions.

For the unreinforced concrete vault, a nonlinear fracture-plastic material model (Červenka et al. 1998, Červenka & Papanikolaou 2008) is assigned to the vault elements, capable of capturing important aspects of concrete behaviour such as cracking, crushing, and crack closure. On the contrary, the reinforced concrete footings and invert are modelled using an elastic isotropic material (concrete elastic properties), since cracking in these regions is generally not expected due to the presence of reinforcement. An alternative approach would have been to model the above regions either with explicit or smeared reinforcement, however this would have led to increased computational demands without considerable benefit.

Boundary conditions between the tunnel lining and the surrounding rock-mass are modelled following the familiar Winkler spring approach (Dutta and Roy 2002). Specifically, unilateral compression-only, linearly distributed springs are applied along the vault and the foundation (footings/invert) outer boundary (Fig. 3). The spring compression stiffness (K_V) is calculated considering plane strain conditions, as follows:

$$K_V = \frac{E_s}{1-\nu_s^2} \text{ (kN/m}^2\text{ = kN per meter of spring contraction per meter of line length)} \quad (1)$$

where (E_s) and (ν_s) are the subgrade reaction modulus and Poisson's ratio of the rock mass, respectively. Furthermore, the horizontal friction between footings and underlying rock mass is modelled with elastic bilateral springs of stiffness K_H, typically equal to 30-50 % of K_V (Fig. 3, left).

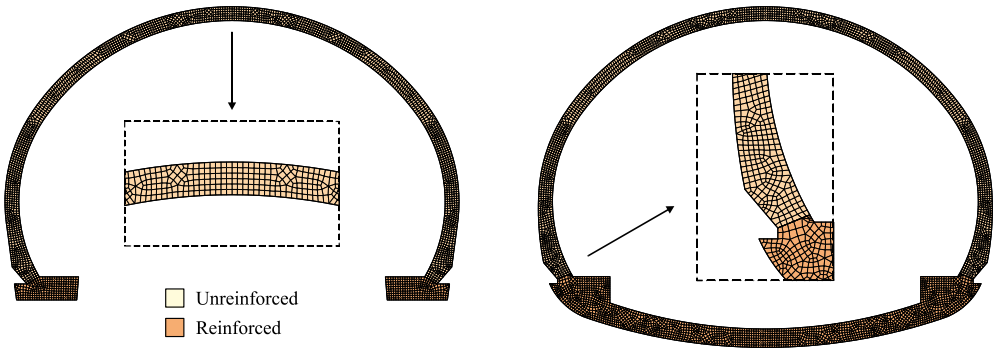

Fig. 2 Finite element meshes : horseshoe section (left) and closed section (right).

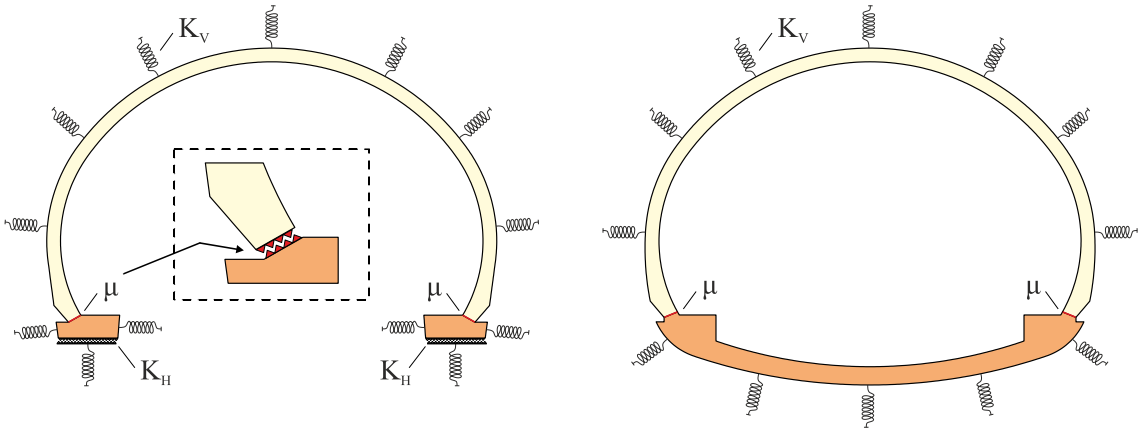

Fig. 3 Boundary conditions between tunnel lining and surrounding rock mass.

Another important modelling aspect is the consideration of the construction joints between the vault and the foundation. These joints are modelled using interface elements, connecting the adjacent vault and foundation line boundaries. The interface elements are configured as unilateral contacts, incorporating a concrete-to-concrete friction coefficient (μ), which depends on surface roughness (typical value 0.8). It is noted that contact modelling is prone to introducing instabilities in the numerical solution and should be handled with caution. To improve stability, it is recommended to use a low value of cohesion (e.g. 0.1 kN). In general, a preliminary geometrically-nonlinear analysis with elastic material properties is recommended, in order to identify and overcome any modelling pitfalls.

2.2 Modelling of various load types

In the following subsections, various load types and load combinations describing static, quasi-static, environmental, accidental, fire, and seismic loading on unreinforced concrete tunnel linings are described, with specific reference to the aforementioned finite element models.

2.2.1 Static, quasi-static, environmental, and accidental loading

The first load case that develops after construction is the lining dead load, defined as a gravitational body load automatically calculated from finite element tributary areas, on the basis of the density of concrete (typically $\rho_c = 2400$ kg/m^3 for normal unreinforced concrete). This is followed by the development of early creep effects, which can be simply represented by an equivalent uniform temperature decrease ($-\Delta t$) in concrete finite elements. A similar load type is subsequently applied to account for environmental temperature variations, usually during winter (typically $\Delta t = -10$ °C in southern Europe). Furthermore, pavement and traffic (on the invert's top boundary) live loads are applied in the form of a constant distributed force, as depicted in Fig. 4. The last case in the above sequence is the external rock mass load, which gradually develops in a long term fashion, after the excavation and construction of the tunnel, depending on the physical properties of the rock mass (higher values correspond to more deteriorated rock mass). This may be represented by a linearly varying distributed force, normal to the tunnel lining, with an upper bound of p_1 at the vault key and a lower bound of p_2 at the vault base (Fig. 5), further decreasing to zero at the invert floor. The aforementioned sequential application of static, quasi-static and environmental loads is considered as the *basic combination* (also referred to as *sequence*) for the assessment of the tunnel structural response.

A special situation that also has to be assessed is the tunnel structural integrity at the time of formwork demoulding. This can be conveniently modelled by modifying concrete material parameters, in order to reflect the concrete strength at the time of demoulding (usually a small fraction of the 28-day strength). This updated dead load case should be subsequently followed by the application of hydration heat, in the form of uniform temperature increase ($+\Delta t$) in concrete finite elements.

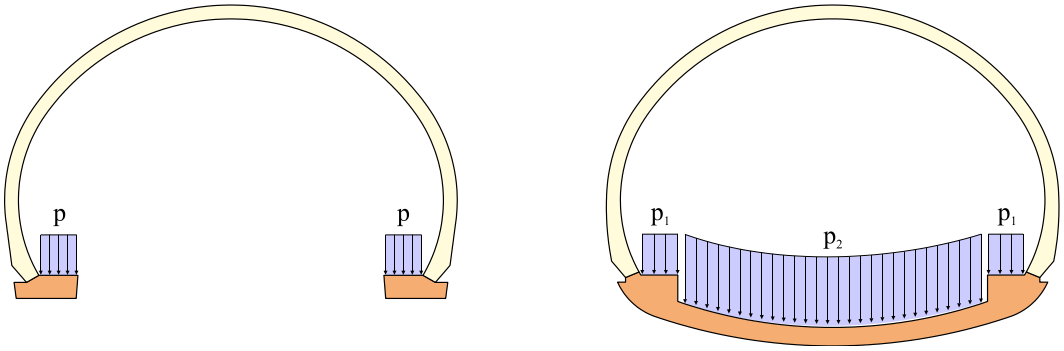

Fig. 4 Application of pavement load.

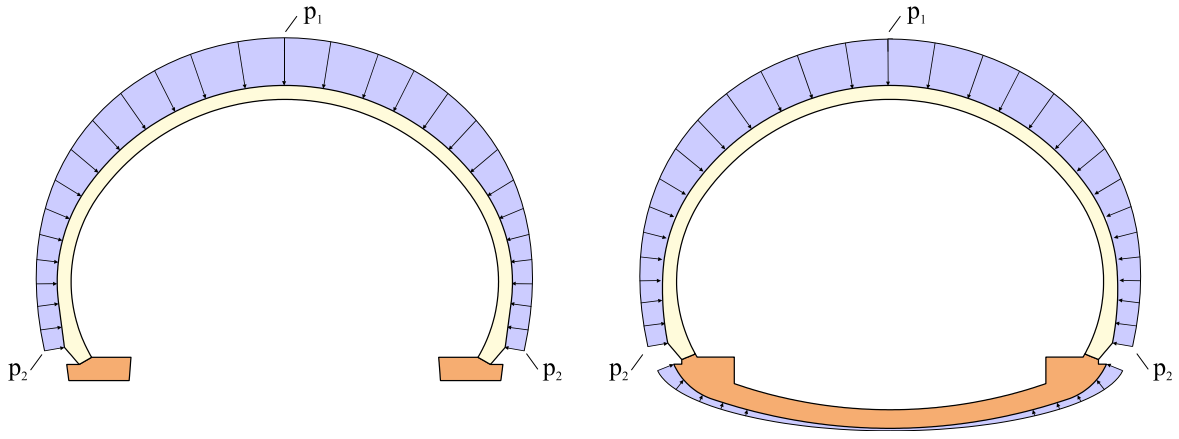

Fig. 5 Application of rock mass load.

Accidental loading is another important case that should be addressed in design or assessment of tunnel linings. Three accidental load cases are described hereinafter, namely blast, hydrostatic, and wedge loading, which should be properly combined with the aforementioned static and environmental loads before analysis:

(a) Accidental hydrostatic loading (due to possible blocking of the drainage pipe next to the construction joint) is modelled using a horizontal triangularly distributed force on the blocked side of the lining (Fig. 6, left). The load value at the base is $p = \rho_w \cdot g \cdot h$, where ρ_w is the density of water (1000 kg/m^3) and h is the vault height. This case succeeds the [dead + creep + pavement + rock mass] load sequence in the analysis.
(b) Blast (explosion) loading is modelled using a constant inverted distributed force on the inner lining boundary (Fig. 6, right). This case succeeds only the [dead + creep] load sequence in the analysis for safety, since it counteracts both environmental and rock mass loading.
(c) Wedge loading is a special case that emerges from the accidental abruption of large rock volumes from the tunnel surrounding rock mass, forming blocks ('wedges') as shown in Fig. 7 (left). The tendency of the wedge to detach from the surrounding rock mass will trigger an arching effect in the initial stress field above the wedge; in other words the 'void' (the discontinuity) created in the rock-mass due to the detachment of the wedge will magnify the stresses on either end, causing a local overstressing in these areas. This can be modelled by modifying the aforementioned rock mass load case (Fig. 5) as follows: by operating only on the half-length of the vault (from key to construction joint), the rock mass load is augmented in both half-length ends (p_3) and reduced in-between (p_4). The augmentation length is expressed as a fraction (α) of the total half-length (ℓ) and controls the severity of the wedging effect. Typical values for (α) are in the range of 0.2 ~ 0.3. The wedge case succeeds the [dead + creep + pavement] load sequence in the analysis.

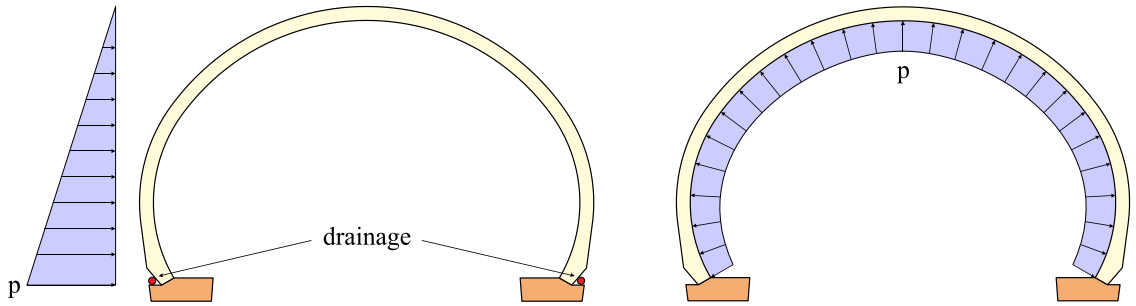

Fig. 6 Application of hydrostatic (left) and blast loading (right).

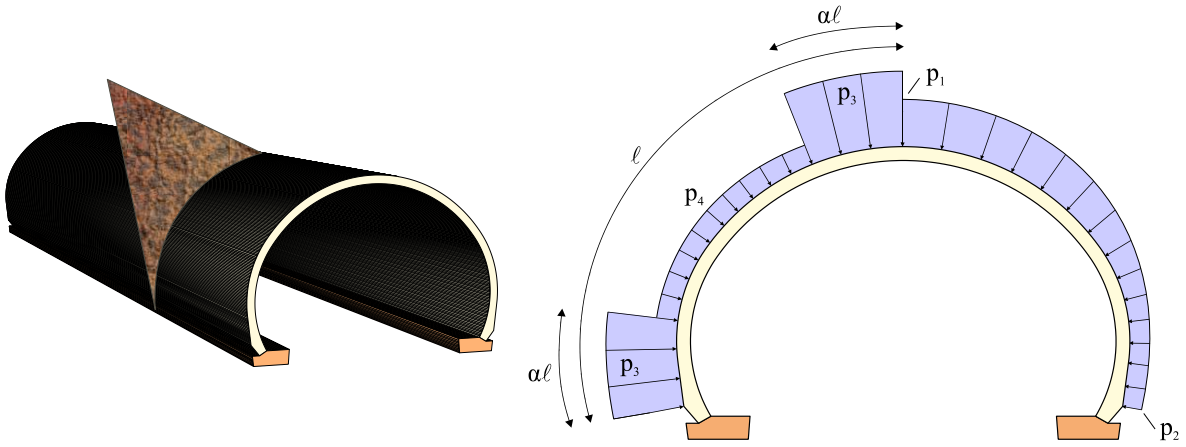

Fig. 7 Rock volume abruption (left) and application of wedge loading (right).

It is finally noted, that for carrying out the nonlinear analysis, an adequate number of load steps (typically 20) is assigned for each load case participating in the load sequence. The solution algorithm employed is a standard Newton-Raphson scheme with line searches, since snap-through and snap-back phenomena (i.e. concrete softening) are generally not expected herein. The convergence criteria of the solution algorithm should be carefully selected, to maintain balance between numerical stability and computational cost.

2.2.2 Fire loading

The structural response of the unreinforced concrete tunnel linings under fire is a special accidental loading type that requires extensions and modifications to the former conventional nonlinear analysis practices, mainly in the aspects of finite element modelling, material constitutive models and solution procedures (Červenka et al. 2004, Bergmeister 2008). More specifically, the analysis procedure is currently twofold; a heat transfer (transport) analysis based on a specific temperature profile is first performed, providing concrete strain fields vs. fire exposure time. These calculated strain fields are subsequently injected into a nonlinear static (mechanical) analysis, which provides concrete stress and cracking evolution during fire exposure. It is assumed for simplicity that the two aforementioned analysis procedures are uncoupled.

In order to conduct heat transfer analysis, it is advisable to first densify the finite element mesh along the fire front line to provide higher resolution in the strain field results that will be introduced in the ensuing static analysis (Fig. 8). Furthermore, to avoid potential numerical instabilities during static analysis, the fire front is marginally shifted away from the construction joint interfaces. The material heat transfer model employed, assigned to concrete finite elements (Červenka et al. 2012) is an advanced heat and moisture diffusion model that requires the following parameters:

(a) Concrete type (siliceous or calcareous).
(b) Concrete water-to-cement ratio (w/c).
(c) Concrete thermal conductivity (λ_c) vs. temperature (T).
(d) Concrete volumetric specific heat (c_V) vs. temperature (T).

The evolution of the thermal conductivity (λ_c) and volumetric specific heat (c_V) for concrete are defined according to Eurocode requirements for fire design (EN1992-1-2 2004b) and depicted in Fig. 9. To be on the safe side, the lower limit of the λ_c - T curve is considered. Subsequently, the fire boundary line (see Fig. 8) is associated with a temperature profile, i.e. the evolution of temperature vs. fire exposure time. Since the pertinent Eurocode, EN1992-1-2 (CEN 2004b) does not include explicit recommendations for tunnel fire loading, the employed fire scenarios are selected from the literature (FIT 2005, UPTUN 2008, *fib* 2008, 2010). More specifically, two profiles are selected (Fig. 10), the 'standard' curve (Einheitstemperaturkurve - ETK) of EN1991-1-2 (CEN 2002) and the hydrocarbon fire (modified hydrocarbon curve - mHC), representing the most unfavourable scenario, both operating on a total exposure period of three hours (180 min). The coefficient of heat transfer by convection (α_c) is taken equal to 25 and 50 W/m^{2}·^{o}C for ETK and mHC profiles, respectively, and the emissivity (ε_r) as constant, equal to 0.7 (EN1992-1-2 2004b). The convection and emissivity heat flux is calculated as follows:

$$q_n = \alpha_c \cdot (T_g - T_b) + \varepsilon_r \cdot \sigma \cdot (T_g^4 - T_b^4) \quad (2)$$

where:

- q_n is the heat flow at the fire exposed boundary (W/m^2)
- σ is the Stefan-Boltzmann constant ($5.67 \cdot 10^{-8}$ W/m^{2}·^{o}C^4)
- T_g is the absolute temperature of radiation source (^{o}C)
- T_b is the structure boundary temperature (^{o}C)

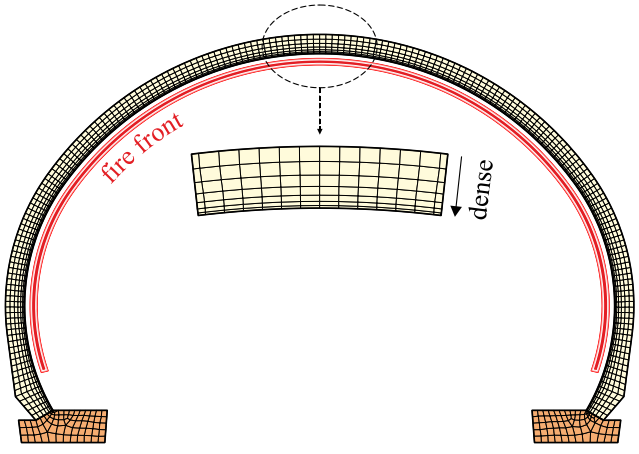

Fig. 8 Vault mesh modification for heat transfer analysis.

The strain fields calculated from the above heat transfer analysis, are imposed on the original model, following the application of the [dead + creep + pavement + rock mass] load sequence. Since concrete properties are temperature-dependent, they are herein introduced as variables (rather than constants) in the nonlinear static problem, following EN1992-1-2 (2004b) and specific software recommendations (Červenka et al. 2012). Variables include concrete elastic modulus (E_c), compressive strength (f_c), tensile strength (f_t), plastic strain (ε_{cp}), fracture energy (G_F) and compressive failure displacement (w_d), in ratio form with respect to normal (15 ^oC) temperature (Fig. 11). The nonlinear static analysis is finally performed using a fine load step corresponding to 15 and 30 seconds of fire exposure (total 720 and 360 steps) for mHC and ETC curves, respectively. It is also possible to account for uneven step size, to optimize the computational cost.

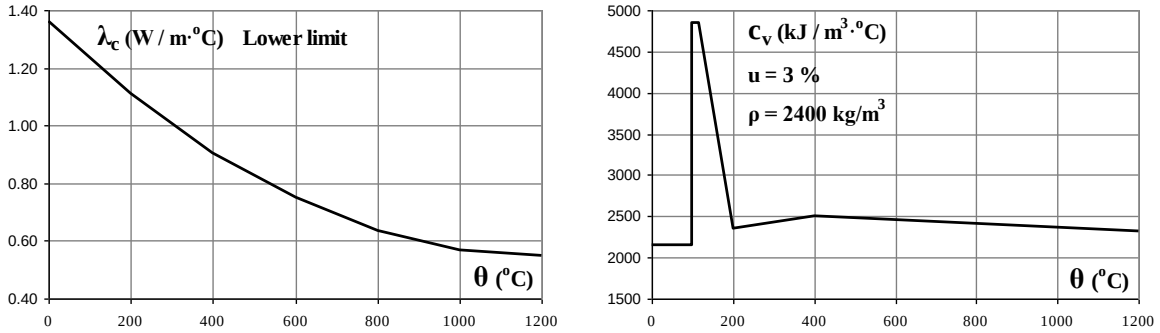

Fig. 9 Evolution of thermal conductivity and volumetric specific heat of concrete vs. temperature according to EN1992-1-2.

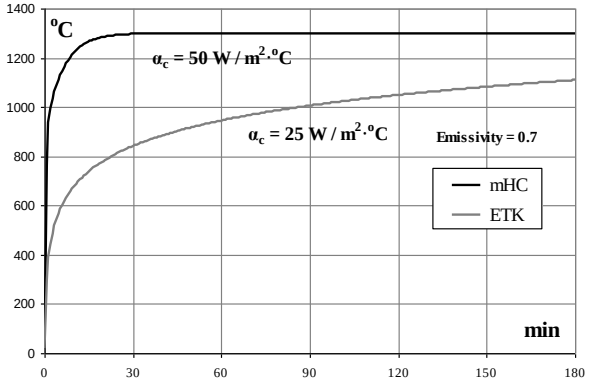

Fig. 10 Fire temperature profiles.

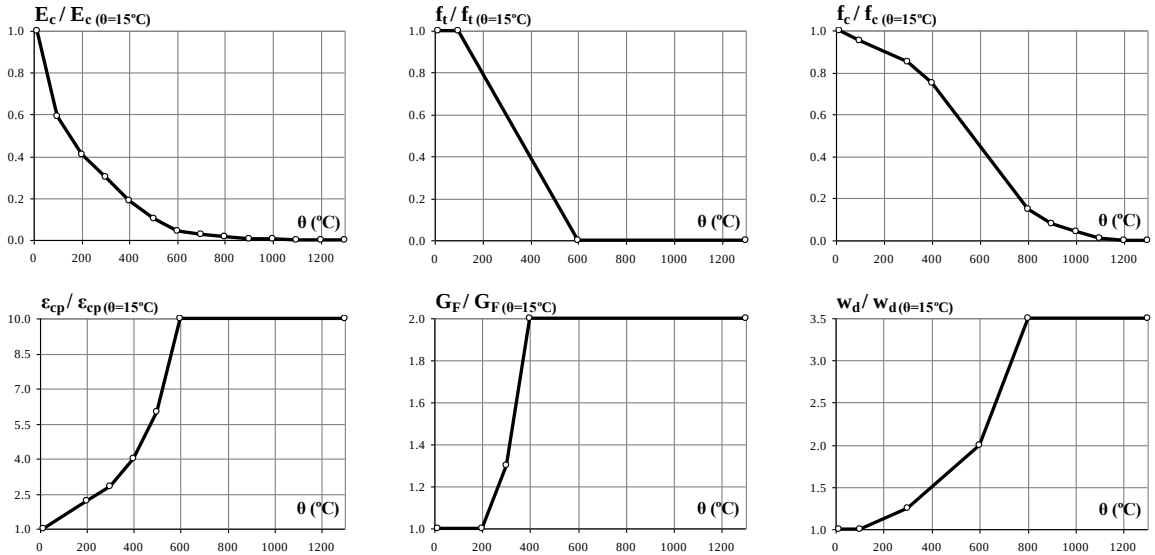

Fig. 11 Temperature-dependent concrete properties.

2.2.3 Seismic loading

In countries of high seismicity, engineering experience has shown that seismic excitation in the vicinity of a tunnel may cause considerable structural damage (Dowding and Rozen, 1978, St. John and Zahrah 1987, Wang 1993), especially to unreinforced concrete linings. Consequently, the trend in international codes of practice (Hashash et al. 2001) is to design tunnel linings against axial strains and curvatures imposed by the surrounding rock mass (where it can be assumed, for simplicity, that the lining strains are practically identical with those of the adjacent rock mass, i.e. the seismic shear wave medium), as well as against shape change (caused by shear deformation of the ground), also referred to as *ovalization*.

Consequently, the final load type investigated in the present study is the seismic excitation of the tunnel lining, a situation that is often overlooked in similar studies due to the complexity involved in its modelling and the associated high level of uncertainty. Two modelling procedures regarding rock mass representation are suggested herein, one for the aforementioned rock mass loading leading to curvature of the longitudinal axis of the lining, which is based on the Winkler spring approach presented in previous sections, and the other for shape change loading, following the more demanding elastic continuum modelling approach.

The first procedure is based on the same models already described for nonlinear static analysis. In line with the plane strain assumption, the seismic loading is applied to the lining section (Fig. 12, left) as a horizontal body load (asymmetrical), which is automatically calculated from finite element tributary areas using the specific weight of concrete, multiplied by the seismic coefficient (a). The seismic coefficient is usually provided from National Annexes to Code regulations (e.g. EN1998-1 2004c), corresponding to the seismic zone where the structure is situated, while here it was estimated from a site-specific seismic hazard analysis (EAEE SA internal report by Pavlidis et al., Dec. 2010). Furthermore, a symmetrical seismic load, mainly resulting from vertical ground shaking, is also considered, acting simultaneously on both sides of the vault. This is realized by applying earth pressure loads at rest, suitably amplified to account for seismic excitation (e.g. $p_1 = 1.5 \cdot \alpha \cdot \rho_c \cdot g \cdot h$, $p_2 = 0.5 \cdot \alpha \cdot \rho_c \cdot g \cdot h$, where (h) is the vault height, Fig. 12, right). Similarly to fire loading, seismic loads are applied subsequent to the [dead + creep + pavement + rock mass] load sequence. This loading case is generally not critical for tunnels bored into rock, but it is included herein for the sake of completeness, since it can be a critical case in other tunnel types (like cut-and-cover).

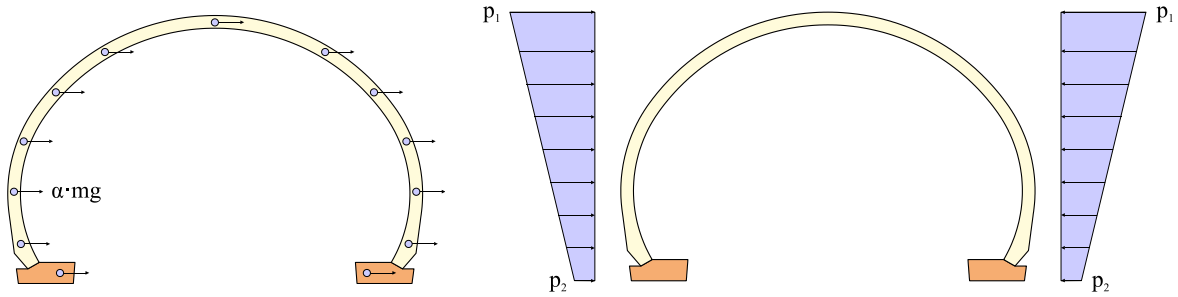

Fig. 12 Asymmetrical (left) and symmetrical (right) seismic loading for Winkler spring models.

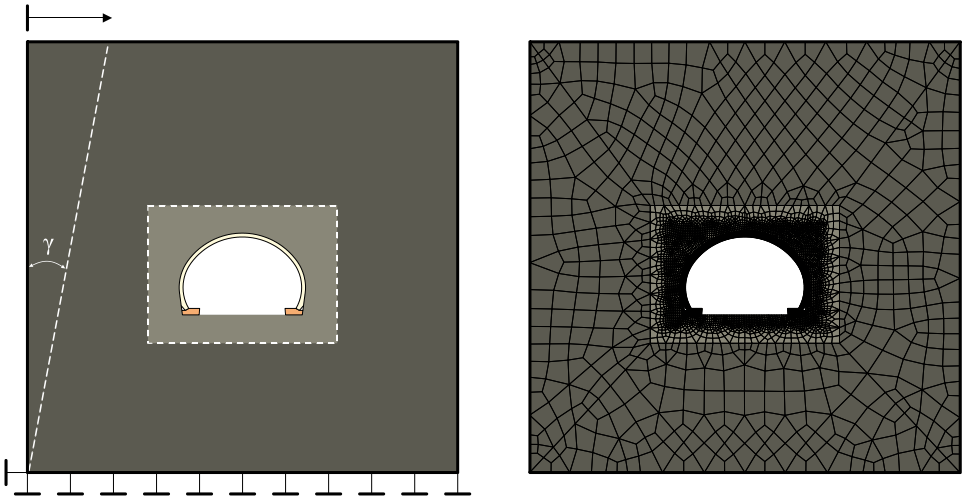

Fig. 13 Ovalization loading (left) and rock mass modelling as elastic continuum (right).

The second and computationally more demanding approach is modelling the ovalization effect due to the shape change imposed by ground deformation caused by seismic excitation. The ovalization load can be represented by a maximum shear distortion (γ) of the ground (Fig. 13, left). The shear distortion value can be calculated as (St. John and Zahrah 1987, Wang 1993):

$$\gamma = V_S/C_S \tag{3}$$

where (V_S) is the maximum expected particle velocity from shear wave and (C_S) is the effective shear wave propagation velocity. This requirement inevitably requires the finite element representation of the surrounding rock mass. To this purpose, an adequately large rock mass profile (50×50 m), corresponding to 3~5 times the tunnel gross dimensions is superimposed on the original model, using elastic isotropic material corresponding to the rock mass elastic properties (see Eq. (1)) as depicted in Fig. 13, right. To optimize the computational cost, the mesh topology of the elastic continuum is described by a smooth transition from the (original) very dense lining mesh to a sparse discretisation at the model boundary. For this reason, two different meshing zones are employed (depicted with different colour in Fig. 13).

As far as the new boundary conditions are concerned, the original distributed springs along the vault outer boundary are removed and replaced by unilateral contact interface conditions (without friction), corresponding to the waterproofing membrane placed between concrete and rock mass (or temporary lining, in other cases) during construction (Fig. 14). However, the horizontal friction between footings and underlying rock mass is preserved. During nonlinear analysis, the dead and creep load are first imposed with restrained model boundaries, followed by the application of shear distortion (γ) profile on the vertical model boundary (using prescribed displacements) and the restraint of the horizontal base (Fig. 13, left). It is finally noted, that a simple and advisable validity check for the integrity of the continuum model, is the comparison of the vault key vertical displacement due to (the same) gravity load, between the continuum and the Winkler spring model. In the present application, a small difference of 5 % was found, which is justified by the fact that springs can contract independently of each other, which does not apply in a continuum model (Dutta and Roy 2002). Nevertheless, this small difference implies that the application of the spring approach on the other case studies presented in this paper is acceptable, let alone the substantially lower computational cost required, which is convenient for practical applications.

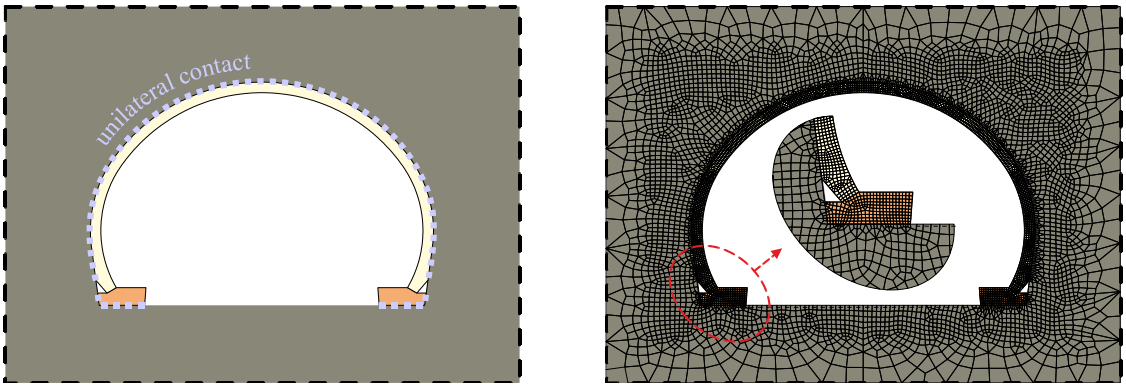

Fig. 14 Boundary conditions between tunnel lining and rock mass.

In the next section, the aforementioned modelling techniques are applied to actually constructed tunnels in the region of central Greece with detailed reference to the pertinent constitutive model and loading parameters, followed by the presentation and discussion of selected nonlinear analysis results.

3. Case studies and discussion of analysis results

In this section, various case studies and representative nonlinear analysis results, based on actually constructed tunnels in central Greece (PATHE project, Maliakos-Kleidi section), will be presented and discussed. These case studies are based on two different lining geometries (see Fig. 1) and various load cases/combinations, as described in the previous section. The verifications are carried out with the aid of both inelastic (nonlinear FEA) and material-elastic analysis methods, while several criteria are checked, as prescribed by codes and/or international recommendations. A detailed list of the considered concrete and rock mass material properties, as well as of load magnitudes, for various load cases are presented in Tables 1 and 2, respectively. The basic,

demoulding and blast combinations are applied to both the horseshoe and closed-section models, while the hydrostatic, wedge, fire, and seismic load combinations are applied to the horseshoe model, corresponding to a lining constructed in a different location (different ground properties). Note that the seismic acceleration was defined on the basis of the previously mentioned site-specific seismic hazard analysis for the site of the tunnel analysed, while the shear strain was estimated from the acceleration and the properties of the rock mass, using empirical relationships from the literature.

Table 1. Concrete and rock mass material properties

Concrete	Units	Load case type			
		Demoulding	Static	Accidental/Seismic	Fire
E_c	GPa	32	32	32	32
ν	–	0.2	0.2	0.2	0.2
α_{cc} , α_{ct}	–	0.85	0.85	0.85	1.0
γ_c	–	1.2	1.5	1.2	1.0
f_{ck}	MPa	2	30	30	30
$f_{cd} = \alpha_{cc} f_{ck} / \gamma_c$	MPa	**0.94**	**17.00**	**21.25**	**30.00**
f_{ctm}	MPa	0.48	2.90	2.90	2.90
$f_{ctk,0.05}$	MPa	0.33	2.00	2.00	2.00
$f_{ctd} = \alpha_{ct} f_{ctk,0.05} / \gamma_c$	MPa	**0.18**	**1.13**	**1.42**	**2.00**
G_F	MN/m	$1.191 \cdot 10^{-5}$	$7.241 \cdot 10^{-5}$	$7.241 \cdot 10^{-5}$	$7.241 \cdot 10^{-5}$
ε_c	–	2.20 ‰	2.20 ‰	2.20 ‰	2.20 ‰
$\varepsilon_{cp} = \varepsilon_c - f_{ctm}/E_c$	–	2.17 ‰	1.66 ‰	1.54 ‰	1.26 ‰
w/c	–	–			0.3
$\rho_{c,unreinforced}$	kg/m^3	2400			
$\rho_{c,reinforced}$	kg/m^3	2500			
α	1/°C	10^{-5}			
Rock mass	**Units**	**Lining type**			
		Horseshoe*	Horseshoe**	Closed section*	
E_s	MPa	1000	800	300	
ν_s	–	0.3	0.2	0.25	
K_V (Eq. (1))	MN/m^2	1098.9	833.3	320.0	
K_H	MN/m^2	329.7	416.7	–	
ρ_s	kg/m^3	–	2600	–	

**for basic, demoulding and blast combinations ** for hydrostatic, wedge, fire and seismic combinations*

Table 2. Load values for various load cases

Load case	Units	Values of load parameters	
		horseshoe model	closed-section model
Hydration	°C	$\Delta_t = +15.0$	$\Delta_t = +15.0$
Creep	°C	$\Delta_t = -7.7$	$\Delta_t = -7.7$
Environmental (winter)	°C	$\Delta_t = -10.0$	$\Delta_t = -10.0$
Pavement (Fig. 4)	kN	$p = 10.0$	$p_1 = 10.0$, $p_2 = 33.3$
Rock mass (Fig. 5)	kN	$p_1 = 180.0$, $p_2 = 108.0$	$p_1 = 200.0$, $p_2 = 120.0$
Blast (Fig. 6, right)	kN	$p = 100.0$	$p = 100.0$
Hydrostatic (Fig. 6, left)	kN	$p = 90.0$	–
Wedge-a (Fig. 7)	kN	$\alpha = 1/5$, $p_3 = 270.0$, $p_4 = 36.0$	–
Wedge-b (Fig. 7)	kN	$\alpha = 1/3$, $p_3 = 270.0$, $p_4 = 36.0$	–
Seismic, symmetric (Fig. 12, left)	–	$\alpha = 0.35$	–
Seismic, asymmetric (Fig. 12, right)	kN	$p_1 = 129.6$, $p_2 = 43.2$	–
Seismic, ovalization*	–	$\gamma = \pm 0.006$	–

**from Eq. (3) → $\gamma = V_S/C_S = 0.41/650 \approx 0.006$*

As noted in the Introduction, for unreinforced concrete tunnel linings, the key performance criterion is crack width; this can be checked either indirectly (through simplified material-elastic analysis for bending moment and axial loading, followed by the estimation of natural axis depth), or directly, through advanced nonlinear analysis that permits reliable estimation of crack width. The herein employed analysis software (ATENA, Červenka et al. 2012) is capable of providing both cracking propagation/orientation and corresponding width. Consequently, the assessment of the tunnel lining response under various loading conditions can be primarily performed in terms of (a) maximum crack width and (b) remaining uncracked zone across the lining section thickness at the end of the analysis. The latter can be estimated either from software cracking visuals or from

colour contours corresponding to the initial (uncracked) concrete tensile strength (f_{ctd}) (Fig. 15, left). It is noted however, that a proper estimation of the uncracked zone should not only consider the above reduction of the concrete tensile strength itself but also the actual severity (width) of cracking. For unreinforced concrete, tunnel designers typically use the criterion that crack width should not exceed 1.0 mm, while the remaining uncracked zone should be at least half of the total lining thickness (DIN 1045-1 2000, AFTES 2000).

Since specific recommendations for assessing the nonlinear structural response of tunnel linings are not generally provided in codes of practice, selection of appropriate criteria is required to handle the present problem from a conventional/code perspective, as necessary for comparison and validation reasons. More specifically, the nonlinear finite element analysis is repeated here, considering elastic isotropic material properties (analysis will still be geometrically nonlinear due to boundary conditions), calculating the section *capacity factor* (λ) for different action effects, i.e.:

(a) Flexural capacity ratio ($\lambda_M = M_{Ed}/M_{Rd}$) for a fixed axial load, where M_{Ed} is the moment derived from analysis (integrated from stresses across the lining thickness) and M_{Rd} is the flexural capacity, calculated from material properties and section geometry.
(b) Axial capacity ratio ($\lambda_N = N_{Ed}/N_{Rd}$), where N_{Ed} is the axial force from analysis (compression negative) and N_{Rd} is the axial capacity of the section, calculated as follows (EN1992-1-1 2004a):

$$N_{Rd} = f_{cd} \cdot b \cdot h_w \cdot (1 - 2 \cdot e/h_w) \tag{4}$$

where $e = M_{Ed}/N_{Ed}$ is the section eccentricity (Fig. 15, right), applicable for $h_w/2 > e > 0$, yet with an upper recommended value of $0.3 \cdot h_w$ (AFTES, 2000). In the present application, $b = 1.0$ m and $h_w = 0.45$ m are considered, whereas safety conditions correspond to capacity ratios $\lambda \leq 1$. It is noted, that if concrete cracking does not occur in the initial nonlinear analysis, it is not necessary to repeat the analysis considering elastic material properties.

Other possible evaluation criteria are the vertical deflection at the vault key, the overall section deformed shape and the interface behaviour at the construction joints and concrete-rock mass boundaries (ovalization case). The application of all aforementioned evaluation procedures along with the respective analysis results are presented in the subsequent subsections.

3.1 Static, quasi-static and environmental loading

Fig. 16 shows the analysis results from the basic [dead + creep + temperature + pavement + rock mass] load sequence for both horseshoe and closed section lining sections. The residual concrete tensile strength (f_{ctd}) contours are displayed on the model deformed shape (×50), overlaid by the corresponding cracking pattern. Moreover, the vertical deflection (δ) history at the vault key is depicted, together with the maximum crack width, remaining uncracked zone and equivalent eccentricity, after the end of the analysis.

From the analysis of the basic load combination, it is observed that crack widths and remaining uncracked zones remain well below the acceptable limits (Fig. 16, right). This is also confirmed by the calculated equivalent section eccentricity from elastic analysis, implying that simplified code recommendations may yield reliable estimates in this case when advanced nonlinear analysis is not available. Furthermore, from the vault key deflection history, it is observed that mainly creep and temperature load stages induce larger displacements on the closed-section model due to its geometry. Therefore, it is concluded that for the basic load combination, the overall structural response of the unreinforced tunnel lining is satisfactory.

As far as the demoulding [dead + hydration] load sequence is concerned, which incorporates very low values for concrete strength (see Table 1), negligible cracking and practically zero deflection is observed at the vault key after the end of the analysis, for both the horseshoe and closed-section models. This is justified by the fact that the initial deflection/cracking caused by gravity load is counteracted by the subsequent concrete expansion induced by hydration heat loading (Fig. 17). This favourable response is revealed due to the use of the advanced concrete constitutive model, which can successfully handle crack closure. Consequently, it is considered that the lining response during demoulding remains well within safe limits.

3.2 Accidental loadings (static)

The first accidental load combination analyzed is hydrostatic loading due to possible blocking of the drainage pipe. Analysis is performed on the horseshoe model and results indicate no cracking along the vault section, a small maximum vertical deflection of 6.6 mm (which is 1/2000 of the lining inner diameter, well below any code limits that vary from 1/500 to 1/250 of the span for horizontal straight members), and an equivalent eccentricity of 8.1 cm. This is justified by the fact that hydrostatic loading is concentrated at the vault base and

cannot cause important horizontal deflections (0.48 mm at vault key). Since all evaluation criteria are fully satisfied, it is considered that the hydrostatic combination is of minor importance and can be safely ignored.

On the contrary, under wedge loading, which replaces the conventional rock mass case, considerable concrete cracking is estimated, especially when high (α) ratios are imposed. The considered [dead + creep + pavement + wedge] load sequence is applied on the horseshoe model for two different cases (α = 1/5 and α = 1/3) and analysis results are summarized in Fig. 18. It is observed that whereas crack widths are below allowable limits, the uncracked zone is estimated to be smaller than the minimum allowable value ($h_w/2$). Moreover, cracking is not localized at the vault key bottom fibre, but is also significant at the lateral top fibres as well. Due to asymmetrical loading, an uneven deformed shape is developed, with relatively high values of deflection at the vault key. Therefore, wedge loading is found to be a critical accidental situation, which should be handled with caution in the design and assessment of unreinforced tunnel linings.

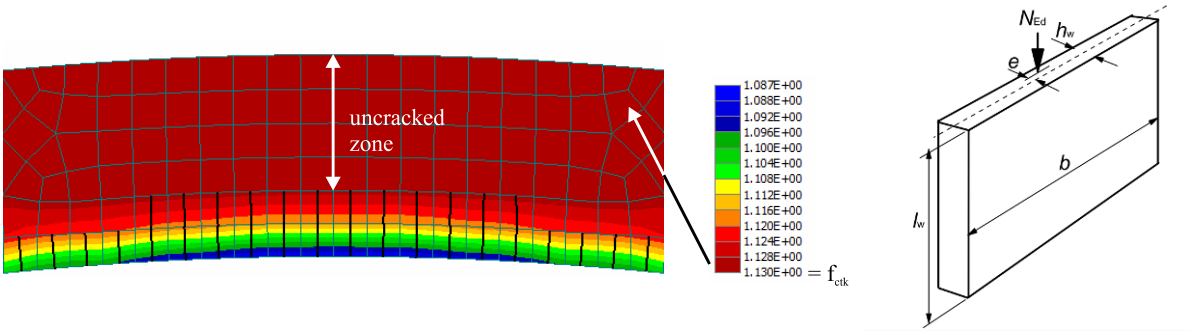

Fig. 15 Approximation of the uncracked zone (left) and definition of section eccentricity (right).

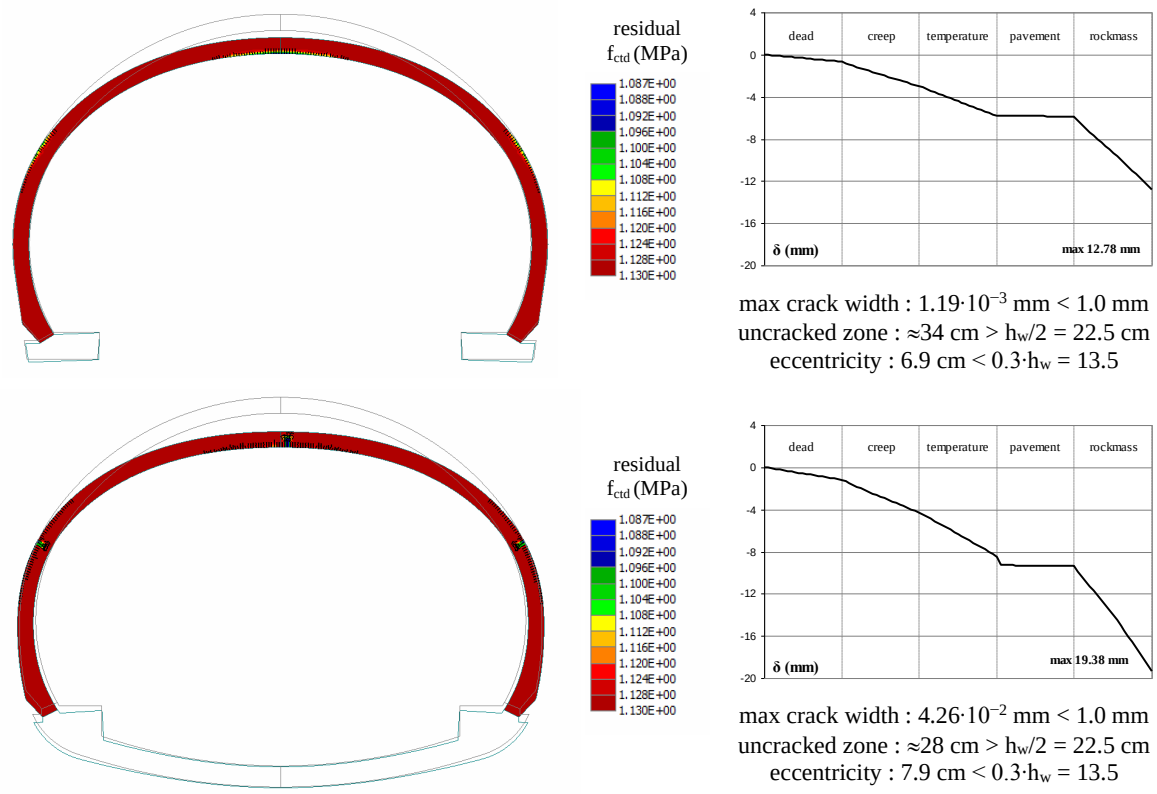

Fig. 16 Analysis results for the basic load combination.

The final accidental case considered is blast (explosion) loading, following the [dead + creep] load sequence. Contrary to intuition, the analysis results do not demonstrate any concrete cracking at all, while vault key deflection is negligible. However, a closer observation of the deformed shape explains this structural response, since a large proportion of the blast energy is released on the gap opening of the construction joints, which are modelled as unilateral contacts with friction (Fig. 19, see also Fig. 3). It is noted that, if a monolithic modelling

approach was followed instead (using a perfect connection between vault and footings/invert), the blast energy would inevitably have been absorbed by severe axial tensile failure of the vault sides, which does not correspond to the actual behaviour of a properly designed lining under blast loading.

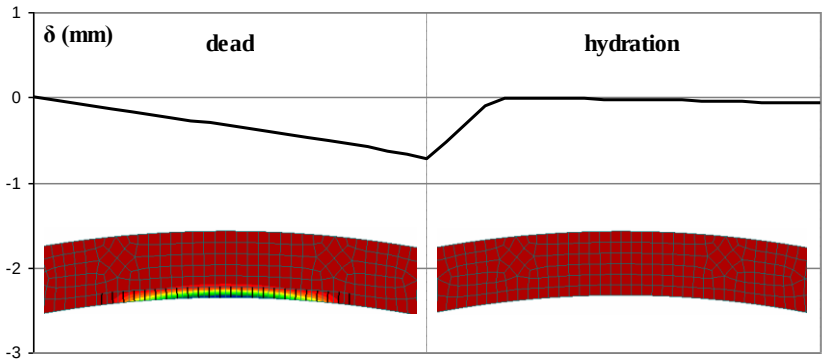

Fig. 17 Demoulding load sequence and corresponding response.

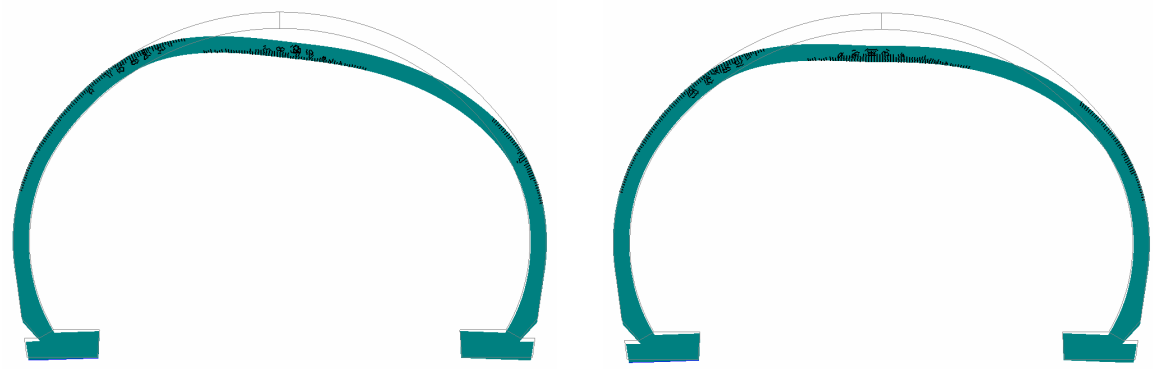

α = 1/5
max crack width : 0.14 mm < 1.0 mm
uncracked zone : ≈7.5 cm < $h_w/2$ = 22.5 cm
max vertical deflection : 15.37 mm

α = 1/3
max crack width : 0.19 mm < 1.0 mm
uncracked zone : ≈7.5 cm < $h_w/2$ = 22.5 cm
max vertical deflection : 17.89 mm

Fig. 18 Analysis results for wedge load combination.

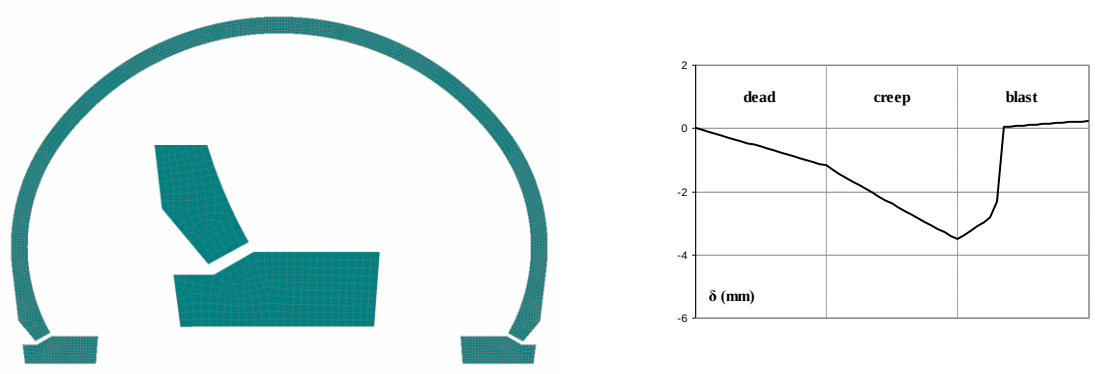

Fig. 19 Analysis results for blast loading combination.

3.3 Fire loading

As already described in section 2.2.2, fire analysis is performed using an initial heat transfer analysis (thermal response), followed by a nonlinear static analysis (mechanical response). For thermal analysis, two different fire

profiles of increasing severity (ETK, mHC) are applied. Fig. 20 shows the evolution of heat transfer using the standard ETK fire curve at the vault key region (response is identical along the entire fire front), for the considered exposure time of three hours (max 1100ºC). It is observed that after the end of the exposure, at least half of the lining thickness remains at initial temperature (15ºC). Similar results are obtained also by applying the mHC profile (max 1300ºC).

Based on the strain fields resulting from the above heat transfer analysis, a nonlinear static analysis with variable (temperature-dependent) material properties is performed, following the initial application of the [dead + creep + pavement + rock mass] load sequence. Fig. 21 shows the residual concrete tensile strength contours during fire exposure, where it is clearly observed that after the fire event, the remaining uncracked concrete regions correspond only to a small fraction of the lining section. This is also visible in the corresponding crack width contours on the same figure, where unacceptable cracking (over 1.0 mm width) is visible along the fire front boundary. Furthermore, in order to evaluate capacity factors according to code recommendations (EN1992-1-1 2004a), analysis is repeated using elastic concrete material with constant properties. However, flexural (M_{Rd}) and axial (N_{Rd}, see Eq. (4)) capacities are calculated considering the variation of concrete strength (f_{cd}) with temperature. Fig. 22 shows the evolution of flexural capacity factor (λ_M), axial capacity factor (λ_N) and eccentricity (e) during the ETK fire exposure. It is observed that all different evaluation factors reach unacceptable limits very early (6~8 minutes of exposure) and therefore it is confirmed that the analysed unreinforced lining section is inadequate to resist standard fire loading. As far as the more demanding hydrocarbon fire curve (mHC) is concerned, it is obvious that the lining response is even worse, exhibiting severe cracking across the entire lining thickness, while simplified assessment criteria exceed the allowable limits after only two minutes of exposure. It is therefore concluded, that the consideration of fire loading is of paramount importance in the design and assessment of unreinforced concrete linings.

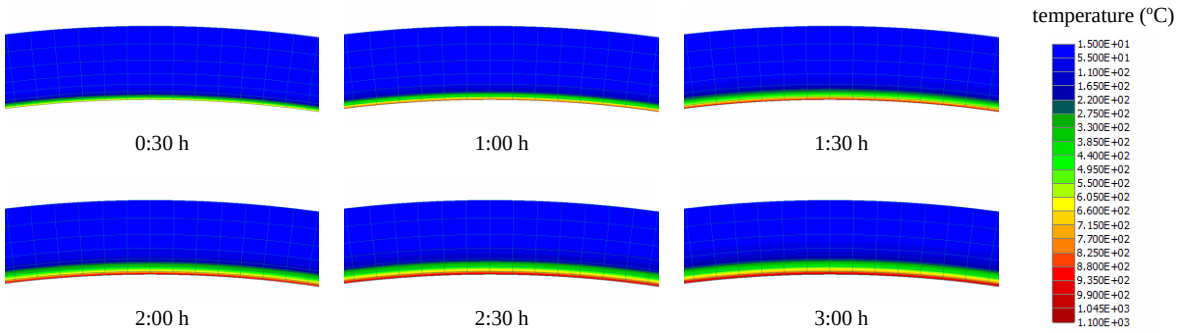

Fig. 20 Evolution of heat transfer at the vault key region for the ETK fire curve.

3.4 Seismic loading

The first two seismic load cases of asymmetric and symmetric loading, used for checking against longitudinal strains imposed by the surrounding rock mass, are applied following the [dead + creep + pavement + rock mass] sequence. From the analysis results, it is observed that these cases do not induce any concrete cracking on the lining section, which is attributed to the strong horizontal resistance of the surrounding rock mass (also observed for hydrostatic loading). Furthermore, calculated eccentricities of 8.5 and 7.3 cm, respectively, indicate that the lining response is well within safety limits. Therefore, it is confirmed that the above cases are not critical for the design and assessment of tunnel linings, especially in a rock terrain (Hashash et al. 2001).

On the contrary, the assessment of the lining response against shape change (ovalization analysis), has yielded interesting results. Considering the rock mass as an elastic continuum surrounding the concrete lining model, the imposed shear distortion (γ) is applied in a cyclic fashion ($\gamma = +0.006 \rightarrow 0 \rightarrow -0.006 \rightarrow 0$), following the dead and creep load cases. Fig. 23 shows the deformed shape (×100) of the continuum model during the application of shear distortion. It is observed that the lining undergoes a considerable shape change, combined with local detachments from the surrounding rock mass, a feature captured due to the direct modelling of unilateral contact interface conditions. Moreover, Fig. 24 shows the principal stress contours (0~0.5 MPa range), where the bearing forces of the rock mass continuum, due to the presence of the lining, are visualised. As far as concrete cracking is concerned, the maximum width value (observed at $\gamma = -0.006$) is equal to 0.73 mm, which is close to the adopted limit of 1.0 mm. Moreover, the depth of the uncracked zone is estimated to be about 5 cm, which is considerably less than the minimum allowable value of $h_w/2$ (Fig. 23, bottom-right).

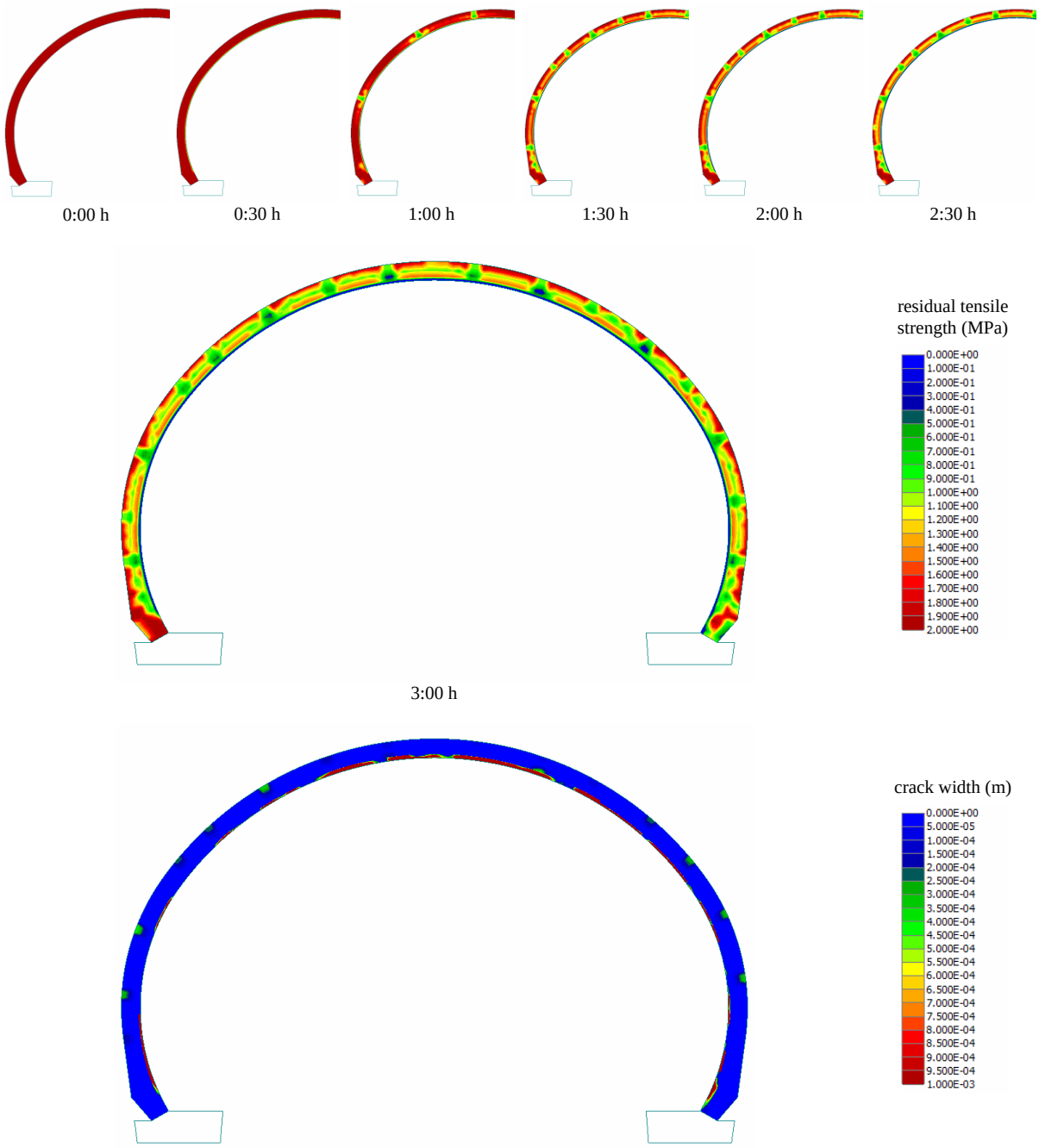

Fig. 21 Evolution of concrete cracking during ETK fire exposure

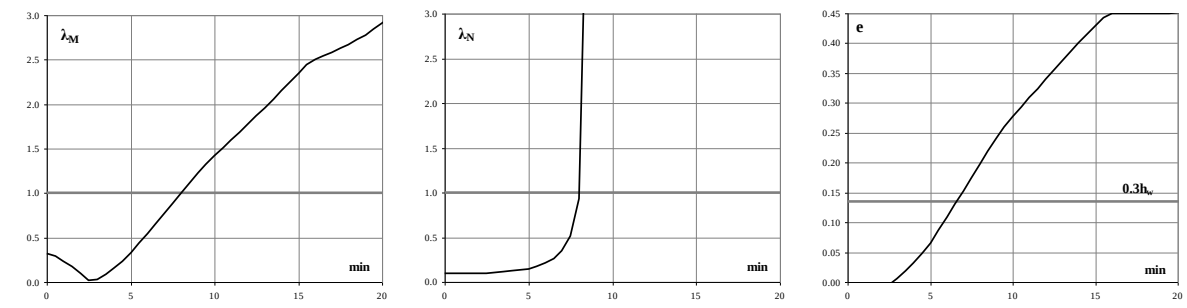

Fig. 22 Evolution of capacity factors (λ_M , λ_N) and eccentricity (e) during ETK fire exposure.

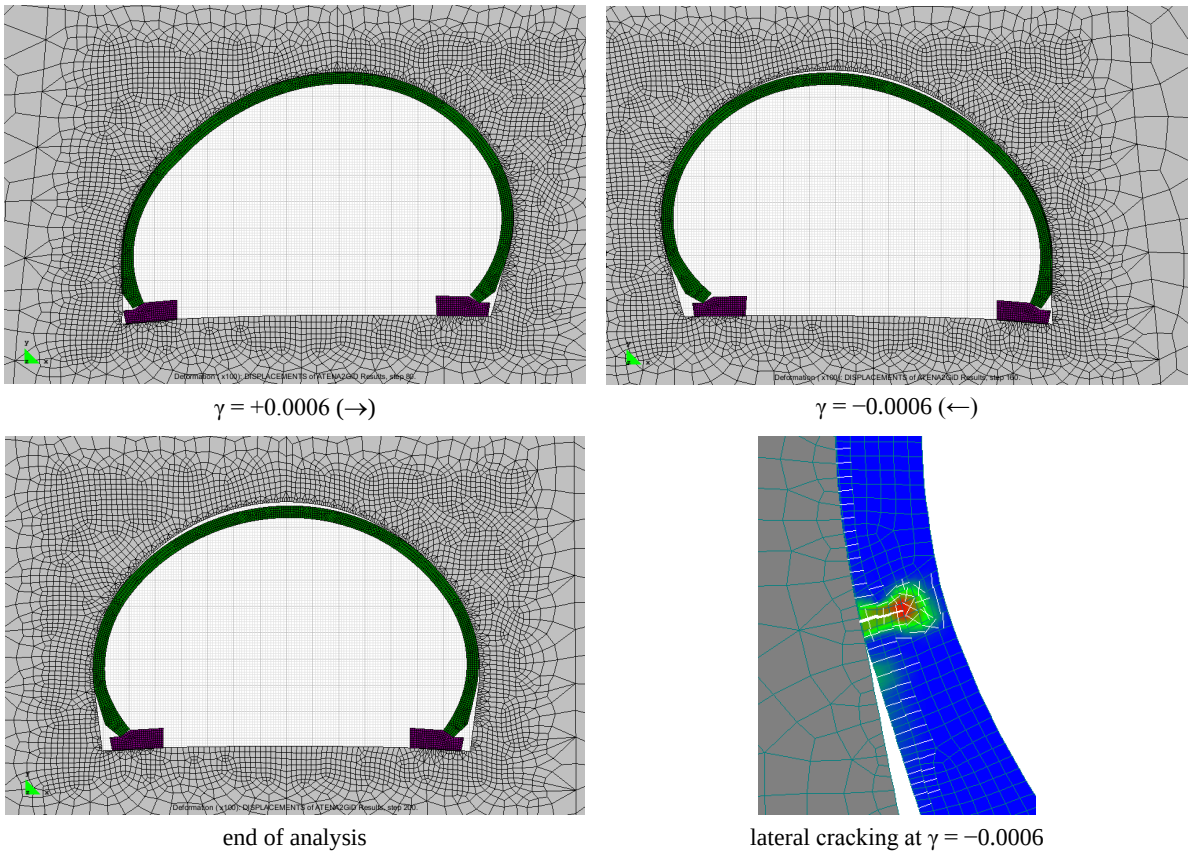

Fig. 23 Model deformed shape and cracking during ovalization analysis.

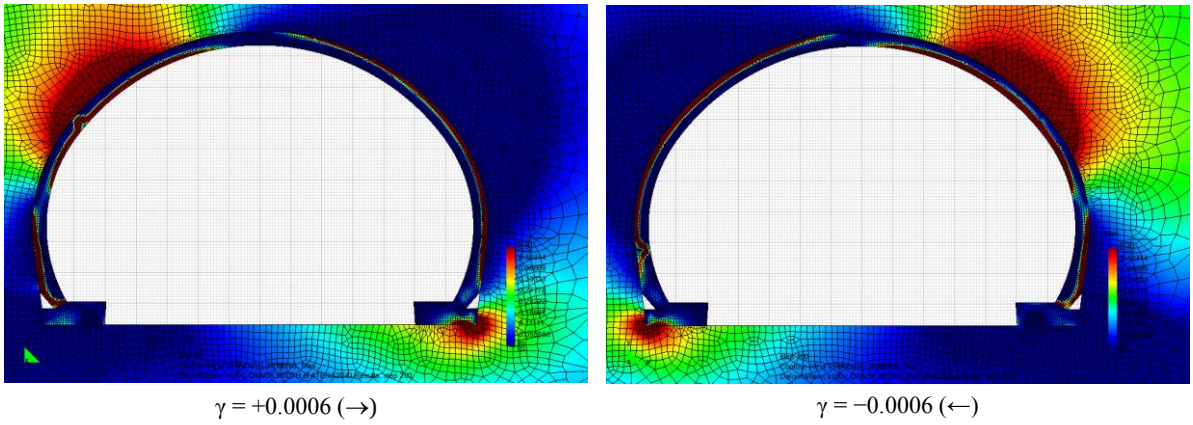

Fig. 24 Principal stress contours of the rock mass continuum during ovalization analysis (undeformed shape).

To further confirm the strong indication of lining section inadequacy due to shape change loading, the maximum section eccentricities during cyclic analysis are calculated. Section inadequacy was observed for all critical loading stages, for instance:

dead+creep $\rightarrow e_{max} = M/N = 8.76/16.93 = 51.7$ cm > 22.5 cm $\rightarrow$ section inadequate
$\gamma = -0.0005 \rightarrow e_{max} = M/N = 64.87/27.29 = 233.7$ cm > 22.5 cm $\rightarrow$ section inadequate

However, it is noted that consideration of the above large eccentricity values, which correspond to relatively low moments and axial loads (e.g. for the dead + creep case), may result in misleading conclusions, regarding the adequacy of the section if cracking has not actually taken place. This issue is also identified in some guidance documents (e.g. AFTES 2000), where the tensile strength of concrete is neglected. For this reason, the

above procedure may be refined by using elastic analysis of the uncracked section (EN1992-1-1 2004a) and checking the tensile stress at the section extreme fibre, as follows:

$$\sigma_{max} = \frac{N}{A} + \frac{M}{I_y} \cdot y \tag{5}$$

dead+creep $\rightarrow \sigma_{max} = 0.30$ MPa $< f_{ctd} = 1.42$ MPa $\rightarrow$ section adequate
$\gamma = -0.0005 \rightarrow \sigma_{max} = 2.00$ MPa $> f_{ctd} = 1.42$ MPa $\rightarrow$ section inadequate

From the additional consideration of the above conventional checks, it is seen that the unreinforced lining section response under shape-change effects induced by seismic loading, can be a critical design situation in earthquake-prone areas and should be duly taken into account.

4. Concluding remarks

The paper identified areas wherein existing codes and guidelines for the design of unreinforced concrete linings need further improvement and/or harmonization. Since the basic design criterion for such linings is the degree of cracking (depth, as well as width, of critical cracks) it appears necessary to provide to the tunnel designer the option of either using advanced analysis methods that result in reliable estimates of the cracking characteristics, or using simplified methods, based on familiar elastic analysis that lead to results that are safe, without being over-conservative.

The finite element analysis procedure described in detail herein is deemed to be useful to designers familiar with the basic concepts of such an analysis, as it provides guidance both on setting up an appropriate model of the lining and the different loads acting upon it, and on interpreting the results of this analysis and expressing them in terms of quantities that allow proper safety verifications (neutral axis depths, axial load eccentricities, crack widths). Comparisons between the key results of nonlinear finite element analysis and those of simplified code-type relationships showed that the latter are generally safe, but often over-conservative, especially when tensile strength of concrete is ignored and limitations on the eccentricity are imposed.

The results of the analysis of the specific common cross-sections (horseshoe and closed) in section 3 of the paper, although strictly applicable to the section geometries studied, are deemed to be of broader interest. In addition to the above conclusions regarding sophisticated and simplified methods, it is interesting to note that the most critical design situations were found to be fire loading (especially the hydrocarbon fire case, which corresponds to the rare, but plausible, case that a lorry carrying fuel is set into fire while crossing a tunnel), and the ovalization of the lining due to seismic ground deformations (note that the case studied here corresponds to a high seismicity area); formation of rock wedges around the tunnel lining could also be a critical situation, albeit less critical than the previous ones, and should be checked in tunnels bored into rock. Last and not least, it was found that among the two typical cross sections studied, the horseshoe section is generally more appropriate than the closed (through an invert) section for unreinforced concrete linings in rock.

Acknowledgements

The authors would like to thank the Egnatia Motorway Company (EOAE SA) for making available to them all the construction drawings of the linings of tunnels T1, T2, and T3 of the PATHE project, as well as the results of the special seismic hazard study for the area (carried out by the team of Prof. S. Pavlidis, from the Aristotle University of Thessaloniki). They would also like to thank Prof. T. Tassios (from the National Technical University of Athens) and Mr S. Raptopoulos (from EAAE SA) for the stimulating discussions of several aspects pertaining to the performance of plain concrete linings, from which this study has benefitted.

References

AFTES [Association Française des Tunnels et de l' Espace Souterrain] (2000), "The Use of Plain Concrete in Tunnels", *Tunnels et Ouvrages Souterrains*, **158**, 110-118.

BASt [Bundesanstalt für Straßenwesen – Federal Highway Research Institute] (2007), "Zusätzliche Technische Vertragsbedingungen und Richtlinien für Ingenieurbauten ZTV-ING, Teil 5 Tunnelbau, (Additional Technical

specifications and guidelines for Civil Engineering Structures ZTV-ING, Part 5 Tunnel Construction)", Report. No. S 1056.
Bergmeister, K. (2008), "Innovative technologies to upgrade fire safety of existing tunnels", *Beton- und Stahlbetonbau*, **103**(S1), 2-9.
CEN [Comité Européen de Normalisation] (2002), "Eurocode 1: Actions on structures - Part 1-2: General actions - Actions on structures exposed to fire (EN 1991-1-2)", CEN, Brussels.
CEN Techn. Comm. 250 (2004a), "Eurocode 2: Design of Concrete Structures - Part 1-1: General rules and rules for buildings (EN 1992-1-1)", *CEN*, Brussels.
CEN Techn. Comm. 250 (2004b), "Eurocode 2: Design of Concrete Structures - Part 1-2: General rules - Structural fire design (EN 1992-1-2)", *CEN*, Brussels.
CEN Techn. Comm. 250 (2004c), "Eurocode 8: Design of structures for earthquake resistance - Part 1: General rules, seismic actions and rules for buildings (EN 1998-1)", *CEN*, Brussels.
Červenka, J., Červenka, V., and Eligehausen, R. (1998), "Fracture-plastic material model for concrete. Application to analysis of powder actuated anchors", *Proceedings of the 3rd International Conference on Fracture Mechanics of Concrete Structures*, Gifu, Japan.
Červenka, J., Papanikolaou, V.K. (2008), "Three dimensional combined fracture-plastic material for concrete", *International Journal of Plasticity*, **24**(12), 2192-2220.
Červenka, J., Surovec, J. and Červenka, V. (2004), "Fracture-plastic model for the analysis of reinforced concrete structures subjected to fire", *Proceedings of the Workshop: Fire Design of Concrete Structures: What now ? What next* ?, Milan, Italy.
Červenka, V., Jendele, L., and Červenka, J. (2012), "ATENA Program Documentation. Part 1: Theory", Červenka Consulting, Prague, Czech Republic.
Corigliano, M., Scandella, L., Carlo G. Lai, C.G, and Paolucci, R. (2011) "Seismic analysis of deep tunnels in near fault conditions: a case study in Southern Italy", *Bull. of Earthquake Engineering*, **9**(4), 975-995.
DAUB [Deutscher Ausschuss für unterirdisches Bauen e.V. – German Committee for Underground Construction] (2007), "Recommendations for Executing and Application of unreinforced Tunnel Inner Linings", *Tunnel* (int. journal of DAUB, D-50827 Köln), **5**, 19-28.
DIN 1045-1(2000), "Tragwe rke aus Beton, Stahlbeton und Spannbeton, Teil 1", *Bemessung und Konstruktion*. Berlin, September 2000.
Dowding, C. H. and Rozen, A. (1978), "Damage to rock tunnels from earthquake shaking". *Journal of the Geotechnical Engineering Division*, ASCE, **104**(2), 175-191.
Dutta, S.C. and Roy, R. (2002), "A critical review on idealization and modeling for interaction among soil–foundation–structure system", *Computers & Structures*, **80**(20-21), 1579-1594.
FHWA [Federal Highway Administration] (2009), "Technical Manual for Design and Construction of Road Tunnels - Civil Elements", *Publication No. FHWA-NHI-10-034*, Washington, D.C.
fib (2008), "Fire design of concrete structures – structural behaviour and assessment", *fib Bull. no. 46*, Lausanne.
fib (2010), "Structural concrete – Textbook (2nd edition)", Vol. 4, *fib Bull. 54*, Lausanne.
FIT [Fire in Tunnels – EU Thematic Network] (2005), "Design Fire Scenarios, Technical Report (Rapporteur A. Haack)", Brussels.
Hashash, Y.M.A., Hook, J.J., Schmidt, B., and Yao, J.I-C. (2001), "Seismic design and analysis of underground structures", *Tunnelling and Underground Space Technology*, **16(4)**, 247-293.
St. John, C.M. and Zahrah, T.F. (1987), "Aseismic design of underground structures", *Tunnelling and Underground Space Technology*, **2**(2), 165-197.
UPTUN [UPgrading Methods for Fire Safety in existing TUNnels] (2008), "WP 2 Fire development and mitigation measures - D211: Fire scenarios and accidents in the past", EU FP5 Contract G1RD-CT-2002-766, www.uptun.net.
Wang, J.-N. (1993), "Seismic Design of Tunnels: A State-of-the-Art Approach", Monograph, monograph7. Parsons, Brinckerhoff, Quade and Douglas Inc, New York.